Nuclear Physics A517 (1990) 533–553
North-Holland

ANTIPROTON ANNIHILATION AT REST ON LIGHT NUCLEI: Rescattering, strange-particle yield and $B = 1$ annihilation

J. CUGNON, P. DENEYE and J. VANDERMEULEN

Université de Liège, Physique Nucléaire Théorique, Institut de Physique au Sart Tilman, Bâtiment B.5, B-4000 Liège 1, Belgium

Received 28 May 1990

Abstract: Recent experimental data concerning antiproton annihilation at rest on light nuclei (^{2}H, ^{3}He, ^{4}He, ^{14}N and ^{20}Ne) are analyzed in order to disentangle the effect of the rescattering from the genuine $B = 1$ annihilation. Particular attention is paid to the deuteron case for which exclusive or semi-exclusive measurements exist. Although some uncertainty is left concerning the proper description of the rescattering process, it is shown that the frequency of $B = 1$ annihilations is of the order of 3–5% at the most. The exclusive measurements for the ^{14}N and ^{20}Ne targets are satisfactorily explained by the conventional intranuclear cascade model. The strange-particle yields are analyzed in detail in relation with a possible strangeness enhancement in the annihilation and its connection to $B = 1$ annihilations. In particular, the Λ yield is overestimated by the intranuclear cascade in the ^{14}N case, whereas the Λ/K_S ratio is underestimated in the ^{20}Ne case. However, it is shown on very general grounds that the Λ/K_S ratio is intimately connected with strangeness exchange in the rescattering process and has nothing to do with a possible strangeness enhancement. It is shown that the latter is rather measured by another combination of the Λ and K_S yields. The experimental data indicate, for all targets from ^{3}He to ^{20}Ne, a *suppression* and not an enhancement (compared to $\bar{p}N$) of the strangeness production in the annihilation. A possible explanation in terms of dynamical selection rules is suggested.

1. Introduction

A much debated question in the present phenomenology of antiproton annihilation on nuclei refers to $B > 0$ annihilations [a $B = n$ annihilation concerns a process in which $(n+1)$ nucleons are implied [1-7]]. Let us readily give the notion of annihilation on several nucleons a more precise meaning. The conventional view of antiproton annihilation on nuclei is that it consists in a first step (primordial annihilation) where the antiproton annihilates on a quasi-free nucleon, emitting pions (and mesonic resonances) essentially with free-space properties, followed by a second step where the annihilation products can interact with the nucleus by scattering and/or absorption (intranuclear rescattering). The whole process transfers to the nucleus a sizeable fraction of the primordial annihilation energy and several nucleons are ejected. By reference to this picture, we will speak of an annihilation on several nucleons whenever the first step, i.e. the recasting of the matter-energy content of the antiproton resulting in meson production, is no longer localized to a single nucleon but implies two or more nucleons. For $B = 1$, for instance, it may correspond,

in a meson picture, to a process relevant of a diagram where an *off-shell* meson is emitted at the annihilation vertex and absorbed at another vertex by a second nucleon [5-7]). In another scheme, one can think of the fusion of two nucleons and the antiproton into a "fireball" akin to a "compound baryon", which will then decay with statistical properties in a similar way as the "$B=0$ fireball" or "compound meson" does in free-space antiproton–proton annihilation [4,8,9]). The $B \geqslant 1$ annihilation mechanism should be contrasted to $B=0$ annihilation in which the annihilation itself implies a single nucleon and the remaining nucleons possibly participate through the mere rescattering of the *on-shell* products of the annihilation.

$B>0$ annihilations have, in particular, been related with an enhancement of strangeness production compared to the usual ($B=0$) antiproton–proton annihilation, and the "large" Λ yields have been cited as a possible or likely signature [2,10,11]). Recently, however, it has been shown that it is not necessary to call for $B>0$ annihilations to explain the strange particle (mainly Λ) rate, intranuclear rescattering allowing to account for the main features of the data [12-14]).

There exists a definite signature of a $B=1$ annihilation in the form of $\bar{p}d \to \pi^- p$ (at rest) [15-17]); as for annihilation on large-A nuclei, the occurrence of delayed fission [18]), which likely results [19,20]) from the formation of a hypernucleus during the rescattering after annihilation, leaves some possible room for a $B=1$ contribution.

In this context, the appearance of data for annihilation *at rest* on ^{2}H and ^{14}N [ref. [17])] on the one hand, on ^{3}He [ref. [21])] and ^{20}Ne [ref. [22])] on the other is interesting. For the first experiment, the set of data includes multiplicity and inclusive spectrum of charged pions and protons, as well as Λ yields; for the second, the K_S and Λ yields have been measured. The fact that the Λ yield is about twice as large in ^{14}N as in ^{2}H and the value $R=\Lambda/K_S \approx 1$ in He and Ne, again raise the question of the possible role of $B>0$ annihilation. It is the main purpose of this paper to critically analyze this possibility.

More radical views on annihilation involving definitely more than one or two nucleons have been proposed [1,2,23]). But we are interested here in annihilation *at rest* and, due to the conditions of low nuclear density in the annihilation zone [24,25]), it seems adequate to limit the considerations to possible $B=1$ annihilations in this case.

Available data are examined in this paper by means of model calculations. In sect. 2, we analyze the deuteron data and try to focus on the rate of $B=1$ annihilations, which turns out to be poorly determined but anyway small. In sect. 3, we study the ^{14}N and ^{20}Ne data by means of the intranuclear cascade (INC) model [see ref. [26]) and earlier references cited therein]. We briefly recall the main ingredients and then apply the model to different aspects of the data: pion and proton spectra, Λ and K_S rates. We show that data on pion and proton spectra and multiplicites are consistent with the standard model with $B=0$ annihilation and nuclear rescattering as described by INC. We emphasize the role of the ω-meson in strange particle

production. We show that the value of the Λ yield measured in N is easily explained by nuclear rescattering after $B=0$ annihilation, but we find that the Λ and K_S rates in Ne are smaller than expected. Sect. 4 presents quite general considerations on the Λ/K_S ratio. We show, that *independently* of any model, this ratio measures the rate of strangeness exchange in rescattering and has nothing to do with a possible strangeness enhancement. Sect. 5 contains our conclusions.

2. Annihilation on deuteron

2.1. PROTON SPECTRA

A nice feature of these measurements [17]) comes from the existence of data on proton spectra for the exclusive channels $\bar{p}d \to 2\pi^-\pi^+ p_s$ and $\bar{p}d \to 3\pi^- 2\pi^+ p_s$. Experimental analysis [17]) reveals two contributions which have been respectively fitted by a Hulthén-like function at low momentum and a Boltzmann-like shape, at large momentum up to ≈ 1 GeV/c. It has been underscored in the same work [17]) that, contrarily to what was suggested in the past [27]), strangeness production is by no means a prerequisite for the presence of a high momentum tail.

We have attempted an analysis of the proton spectrum in $\bar{p}d \to 2\pi^-\pi^+ p_s$ in terms of pion rescattering by proceeding as follows. We have adopted for the spectator nucleon a Hulthén form [28])

$$\Phi(k) = \sqrt{\frac{2}{\pi}}\left[\frac{1}{\alpha^2+k^2} - \frac{1}{(\alpha+\mu)^2+k^2}\right], \tag{2.1}$$

corresponding in r-space to

$$\Psi(r) = e^{-\alpha r}[(1-e^{-\mu r})/r], \tag{2.2}$$

the parameters being chosen to reproduce the wave function obtained with the Paris potential [29]): $\alpha = 0.32$ fm^{-1}, $\mu = 0.56$ fm^{-1}. A rescattering contribution was obtained in the following semi-classical way. Using phase-space generated $\bar{p}N$ annihilation events, we have considered the pions in a random order and decided on the occurrence of rescattering according to the probability [30])

$$P = \sigma(s)\langle r^{-2}\rangle/4\pi, \tag{2.3}$$

where $\sigma(s)$ is the πN scattering cross section at the c.m. energy $\sqrt{s}$ and where $\langle r^{-2}\rangle$ is the average inverse squared relative distance between proton and neutron in the deuteron ($\langle r^{-2}\rangle = 0.292$ fm^{-2}, ref. [29])). The proton momentum is picked at random from the Hulthén distribution. The scattered proton momenta are obtained with the assumption of isotropic scattering (we also use a more realistic angular distribution in second-order polynomial in cos θ, but the results are very similar). The predicted fraction of rescattered protons amounts to 21%, this figure being quite close to the one of the empirical fit [17]). The resulting distribution (direct spectators + rescattered

protons) is shown in fig. 1a. It is seen that the spectrum is obtained quite well. The explanation of the high momentum tail seems therefore essentially to be found in rescattering. There might still be some small room left for an extra contribution at the higher part of the spectrum. We have introduced a component in the form of the phase-space shape of the proton spectrum in $B=1$ annihilations leading to $2\pi^-\pi^+$p. It seems that the data can accommodate a small ($\approx$3%) contribution of that type (see below) but the accuracy is not sufficient to guarantee a definitive conclusion.

Turning to the $\bar{p}d \to 3\pi^- 2\pi^+ p_s$ channel, we expect the same procedure to give a larger fraction of rescattering; indeed, we predict about 48% of rescattering probability (see fig. 1b) and the predicted spectrum does not fit, in accordance with the fact that the empirical fit [16]) gives 21% in the Boltzmann-like shape.

A similar experimental result [31]) was obtained in $\bar{p}$d annihilation in flight ($\sim$1.3 GeV/c) where the fraction of rescattering was found somewhat smaller in

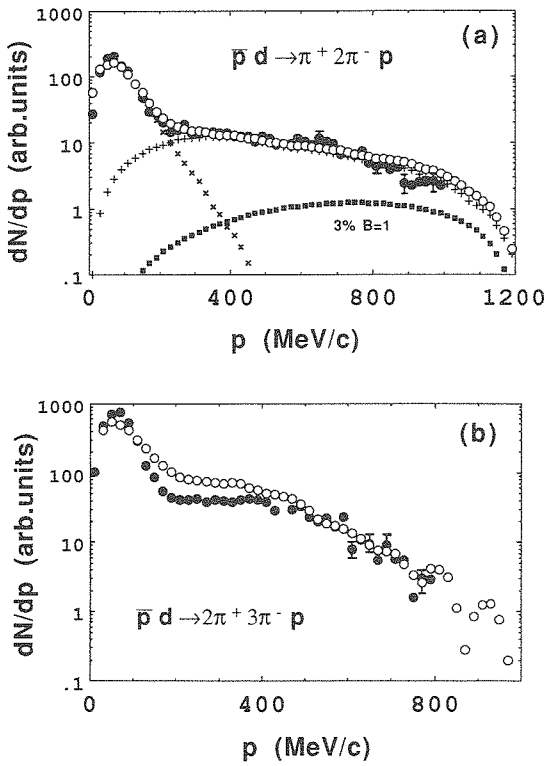

Fig. 1. Proton momentum spectra in two exclusive channels for $\bar{p}$d annihilation at rest. The full dots give the measurements of ref. [17]), for which typical error bars are shown. The open dots give the results of our calculation. For the $\pi^+ 2\pi^-$p channel, the total spectrum is split into its various contributions: no rescattering (×), rescattering (+) for $B=0$ annihilations and $B=1$ annihilations (squares). Both the experimental data and the calculations are normalized on the respective total yields.

events with 5 charged pions (plus any π^0) than with 3 charged pions (plus any π^0). A possible explanation in this case could be the role of the ω-meson, but it cannot be invoked here, since there is no π^0 in the final state. We postpone a discussion on the rescattering to section 2.5. Note, however, that our calculation reproduces fairly well the inclusive proton spectrum provided by ref. [17]), except in the 200–350 MeV/c, where we slightly overpredict it. We have to mention that the efficiency of the detection (completely vanishing under 200 MeV/c) might not be perfect in this range [see ref. [16]) for detail].

2.2. Λ RATE

The measured Λ inclusive rate is $(3.0\pm0.4)\times10^{-3}$ [ref. [17])]. Λ production arises from $\bar{K}$ rescattering only in $B=0$ annihilation. An estimate of the rate is obtained as

$$P(\bar{p}d\to\Lambda X)=P(\bar{p}N\to K\bar{K}X)\langle\sigma(\bar{K}N\to\Lambda X)\rangle\langle r^{-2}\rangle/4\pi, \tag{2.4}$$

where $\langle\sigma\rangle$ is the cross section averaged over the inclusive $\bar{K}$ spectrum. We include, as in the rest of this paper, $\frac{1}{3}$ of the cross section for Σ production to account for Σ^0's which, in the experiment of ref. [17]) as in many others, are indistinguishable from Λ's (we sometimes call these particles $\tilde{\Lambda}$ when we want to insist on this aspect). With $P(\bar{p}N\to K\bar{K}X)\approx5\times10^{-2}$ and $\langle r^{-2}\rangle=0.292\,\mathrm{fm}^{-2}$, the value $\approx1.95\times10^{-3}$ is obtained. Another contribution to Λ production is due to ω, whose yield in $\bar{p}p$ is 0.28 ± 0.11 per event [32]). The calculated Λ momentum spectrum is shown in fig. 2 along with the experimental data of ref. [33]). We also give the contributions of the various channels defined by the number of accompanying pions. Note the importance of the associated production induced by the ω resonance produced in the annihilation. As for the Λ rate, the ω mechanism contributes to 0.89×10^{-3}. There is little room for a $B=1$ contribution, but at a level of less than 3%, as mentioned previously. The latter would contribute to 1.7×10^{-3}. Let us mention that bubble chamber measurements [15]) of $\bar{p}d\to\Lambda X$ gives a larger rate than ref. [17]): $(3.6\pm0.6)\times10^{-3}$.

2.3. RATE OF $B=1$ ANNIHILATIONS

The measured rate [17]) of the channel $\bar{p}d\to\pi^-p$ is $(1.4\pm0.7)\times10^{-5}$. In ref. [8]) a statistical model predicted, for $B=1$ annihilations, branching ratios of 4.7×10^{-4} and 5.7×10^{-2} respectively, for the π^-p channel and for the inclusive $(\Lambda+\frac{1}{3}\Sigma)$ production. From the experimental π^-p rate, we deduce a rate of $(3\pm1.5)\%$ of $B=1$ annihilations; this in turn corresponds to an expected $(1.7\pm0.9)\times10^{-3}$ for the Λ inclusive rate. Note that the two other experimental results for the π^-p channel are $(2.8\pm0.3)\times10^{-5}$ [ref. [16])] and $(0.9\pm0.4)\times10^{-5}$ [ref. [15])]. In view of the large experimental uncertainties one can only conclude that the complete picture is not in disagreement with a contribution of the order of 3% of $B=1$ annihilations but

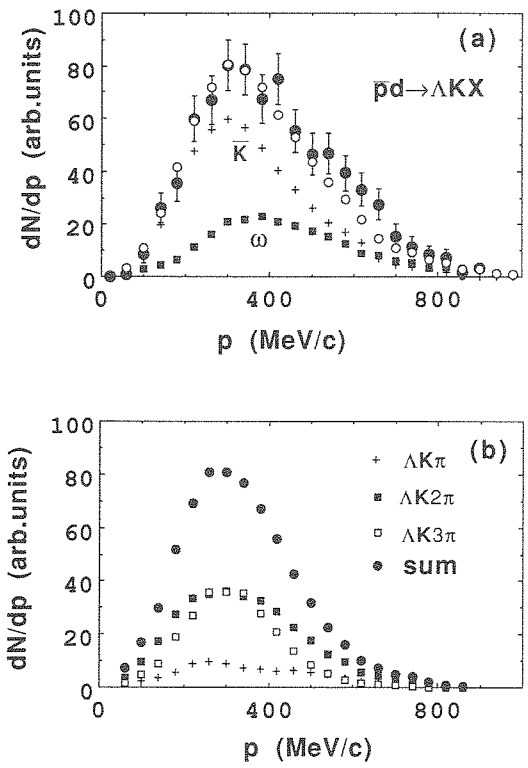

Fig. 2. Inclusive Λ momentum spectrum after $\bar{p}$ annihilation on deuteron (part (a)): experimental data [33]) (full dots), theoretical prediction (open dots), the latter being splitted into the $\bar{K}$ contribution (crosses) and the ω contribution (squares). Part (b) gives the calculated inclusive ΛK yield (full dots, same as the open dots in part (a)) and its most important contributions $\Lambda K n\pi$, $n = 1, 2, 3$. All the curves (theory and experiment) are normalized on the corresponding yields. See text for detail.

that in order to reach a more definite answer it is highly desirable to obtain improved data.

2.4. IMPORTANCE OF RESCATTERING

Above, the $\bar{p}d \to 3\pi^+ 2\pi^- p_s$, $2\pi^+ \pi^- p_s$ and ΛKX have been used in an attempt to infer the $B > 0$ annihilation rate. We have seen that these reaction probabilities are grossly consistent with $B = 0$ annihilation followed by rescattering. If the semi-classical treatment of the latter is valid, $B = 1$ annihilation could be present at the level of a few (3–5) percent. However, the issue will be settled definitely when a precise fully quantum mechanical detailed treatment of the various processes cited above is performed. Apparently, no such calculation exists, except that preliminary results of an approach along these lines by Locher *et al.* have been announced [34]). As far as we can judge, this approach gives roughly the same results as ours for the

ΛKX channel, a smaller rescattering, by a factor ~3, in the $2\pi^+\pi^-p_s$ channel, and even much smaller, by a factor ~10, in the $3\pi^+2\pi^-p_s$ channel. Also, the maximum values of the rescattered proton momentum do not agree with our calculations. These results are really puzzling. Apparently, the strong difference might come from the off-shell propagation of the pions which are rescattered, but the detail of the calculations of ref. [34]) should be known before any conclusion can be drawn. Note that in all the channels which imply pion rescattering, experiments indicate a rescattering probability around 20–25%.

3. Annihilation on N and Ne

3.1. THE INTRANUCLEAR CASCADE MODEL

As it is well known, the INC model is based on the following picture of the annihilation process: the antiproton annihilates on a single nucleon, emitting mainly pions which, travelling through nuclear matter, transfer energy by scattering and/or absorption, possibly ejecting nucleons. The intranuclear interactions are treated in terms of two-body collisions of pions and nucleons, assuming free-space cross sections. The model is fairly successful in the comparison with the bulk of annihilation data and has served up to now as a standard.

For annihilation at rest, the distribution of the annhilation site implies the product of the nuclear density $\rho(r)$ by the density of the Coulomb $(n, l = n-1)$ state [24,25]):

$$p(r) = r^2\rho(r)|\Psi_{n,n-1}(r)|^2 . \tag{3.1}$$

The primordial pionic channels are given by a statistical model which fits the $\bar{p}p$ annihilation properties and the elementary cross sections are essentially taken from experiment.

We have recently used [35,36]) a version of the INC code in which we replace the nucleus constructed as a set of nucleons, each with a position and a momentum, by a continuous distribution; as for the interaction between hadrons, instead of being governed by the motion of disk-like objects along straight segments between collisions, they are determined by mean free path considerations. It has the advantage of much shorter computation times and thus allows to handle rare processes with sufficient statistics. There are some slight differences which are inherent to the methods. In the continuous target case, a struck nucleon is only conferred a particle identity after the collision has taken place; as a consequence, the dependence of the cross section as a function of the c.m. energy of the colliding system is taken into account only in an average way; similarly, the Pauli blocking is introduced by applying an average correcting factor to the $(aN \to bN)$ cross section:

$$\sigma = \sigma_{\text{free}} B(p_f^*) \tag{3.2}$$

with (for isotropic angular distribution)

$$B = 0\,, \qquad \text{if } p_f^* < \tfrac{1}{2}p_F\,,$$
$$B = 1 - p_F^2/4(p_f^*)^2\,, \qquad \text{if } p_f^* > \tfrac{1}{2}p_F\,, \tag{3.3}$$

where p_f^* is the momentum of the final particles in the c.m. system and p_F is the Fermi momentum.

For the rest, the two methods are quite similar. We stress that once a collision has "kicked off" a nucleon from the Fermi sea, this nucleon is treated as a cascading particle; the global cascade is thus made of a superposition of ramified cascades. The main difference between the two methods lies in the absence, in the case of a continuous target, of the "cascade-cascade" interactions, that are, in the other approach, automatically included. There is, however, a strong hint that their role is minimal at low energy [37]). On the other hand, the depletion effect, which is automatically integrated when one deals with individual nucleons should be taken into account. It is the "trawling effect" which has been emphasized in ref. [38]). We have included it in a simple way, which averages the effect over the whole nucleus, by decreasing the nuclear density in the course of the cascade, as

$$\rho(t) = \rho(0) A_{res}/A_{init}\,. \tag{3.4}$$

The procedure is rather crude as it implies, strictly speaking, almost instantaneous rearrangement, but for small nuclei the approximation should be reasonable while for large ones the effect is anyway small.

On the other hand, we have extended the scope of possible studies by using with the mean free path method a number of reactions which are not included in the former code; apart from pions and nucleons, we handle the following particles and their interactions: K, $\bar{K}$, η, ω, Λ, Σ.

3.2. PION CASCADE: PIONS AND NUCLEONS

We have performed first a calculation for the purely pionic part (95%) of the annihilations. The charged pion spectrum and the proton spectrum from N are shown in figs. 3a and 3b. Table 1 summarizes the results concerning multiplicites. The shape of the pion spectrum fits rather well to the data, although there is a small depression in the region of 250–300 MeV/c which is not observed in the data. This kind of discrepancy has been observed in annihilation in flight [26]), where it is more pronounced for a heavy nucleus than for a light one. It can be related to the role of the Δ resonance. The effect is somewhat smaller here for ^{14}N than for ^{12}C in flight, because the number of interacting pions is smaller (1.84 against 2.14 at 600 MeV/c). The mechanism of pion energy degradation might be somewhat less sharply concentrated in a specific band than implied by the isobar interaction with free-space properties incorporated in our model. As for the absorption rate, the predicted value fits the data, which have unfortunately a rather large uncertainty.

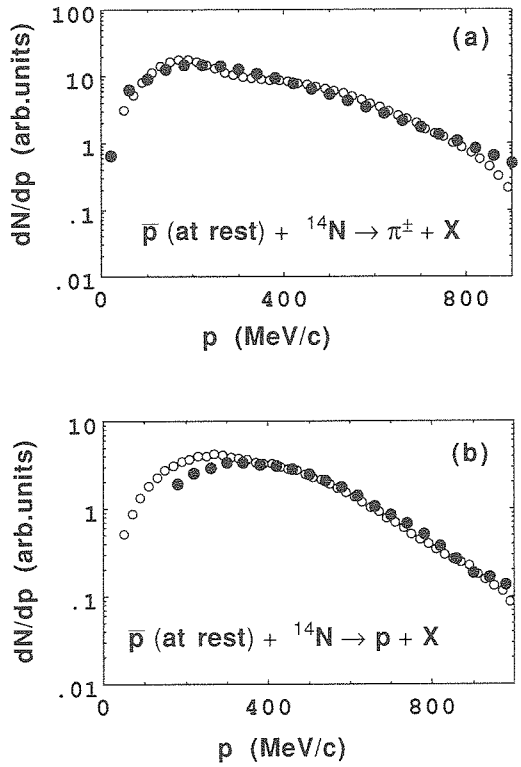

Fig. 3. Comparison between experimental (full dots) inclusive charged pions (part (a)) and proton (part (b)) momentum spectra [17]) for $\bar{p}^{14}$N annihilation at rest, with our INC calculation (open dots). Experimental error bars are typically smaller than the size of the full dots. Both the experimental data and the calculations are normalized on their respective multiplicites. See text for detail.

In fig. 4a, we show our results for the charged pion multiplicity distributions which are also measured in ref. [17]). One can see that the agreement is fairly good, translating the fact that the cascade likely describes correctly the number of collisions per pion.

For the protons, the model essentially overestimates their number at low momenta. We have looked for a possible explanation in the presence of deuterons among the products. An experiment [39]) has found an average of 0.09 deuteron following annihilation on ^{12}C. According to ref. [17]), their experimental set-up does not permit the observation of these ejectiles below 300 MeV/c. We have made an estimate of deuteron emission by using a simple coalescence model [40]). We assume that whenever among the ejectiles a proton and a neutron have momenta which differ by less than a fixed value p_0 they form a deuteron. Taking $p_0 = 130$ MeV/c [ref. [41])], we predict a contribution of 6% of the protons going into deuterons. The predicted deuteron spectrum is shown in fig. 5a where we also show the spectrum of the protons which have built up a deuteron.

TABLE 1

Pion and nucleon multiplicites. The upper part of the table gives the pion multiplicities in $\bar{p}p$ as they are measured or as they are modelled in our calculation. The lower part gives various final particle multiplicites in $\bar{p}^{14}N$ system. The column "INC standard" refers to INC model described in ref. [25]), whereas the column "INC cont." refers to INC model with a continuous medium described in this paper. The last column gives the results when the ω-meson is introduced in the calculation. See text for detail

	Exp. [17])	INC standard	INC cont.	ω
Primordial pions ($\bar{p}p$)				
$\langle\pi^-\rangle$		1.82	1.82	1.85
$\langle\pi^0\rangle$		1.80	1.80	1.83
$\langle\pi^+\rangle$		1.32	1.32	1.42
$\langle\pi^- + \pi^+\rangle$	3.18 ± 0.10	3.14	3.14	3.26
Final pions ($\bar{p}^{14}N$)				
$\langle\pi^-\rangle$		1.69	1.69	1.68
$\langle\pi^0\rangle$		1.67	1.67	1.67
$\langle\pi^+\rangle$		1.24	1.24	1.31
$\langle\pi^- + \pi^-\rangle$	2.89 ± 0.09	2.93	2.93	2.99
$\langle\pi^+/\pi^-\rangle$	0.85 ± 0.08	0.73	0.73	0.78
Nucleons ($\bar{p}^{14}N$)				
$\langle p\rangle$	-	1.05	1.08	1.00
$\langle p\rangle$ (>170 MeV/c)	0.7 ± 0.03	0.88	0.90	0.84
$\langle n\rangle$	-	1.18	1.22	1.12

The deuteron explanation is also consistent with fig. 4b, where the measured proton multiplicity distribution is displayed by the heavy dots. The raw results of the cascade are given by the histograms. In particular the percentage of no proton events is underestimated. The subsequent coalescence of protons with neutrons will inevitably increase this percentage.

3.3. ROLE OF THE ω-MESON ON PION AND PROTON SPECTRA

It is known that $\bar{p}N$ annihilation produces resonances rather copiously. The INC model as used above assumes implicitly immediate decay of the resonances into pions after production. This seems a reasonable approximation for short-lived resonances ($\Gamma > 100$ MeV). Such is not the case, however, for long-lived ones, namely η and ω resonances. We have included the ω meson in our calculation (η's do play a minor role at low energy). This requires some rules for the production and interaction properties. For describing the production, we have added the ω to other particles in the statistical model of ref. [8]) for $\bar{N}N$ annihilation, adapting the interaction volume to keep the final pion multiplicity after ω decay (assuming 100% 3π decay). The mean ω multiplicity turns out to be equal to 0.27, in agreement with the experimental rate [32]). For the interactions of ω, we retain mainly the following

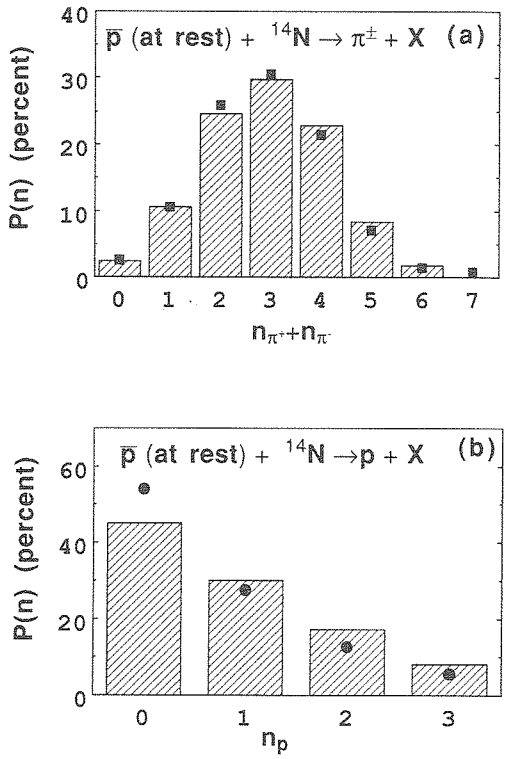

Fig. 4. Charged pion (a) and proton (b) multiplicity distribution for $\bar{p}^{14}N$ annihilation at rest. The symbols (squares and full dots) correspond to the data of ref. [17]). Experimental error bars are smaller than the size of the symbols. The histograms are the results of our calculation.

possibilities:

$$\omega N \to \omega N\,, \tag{3.5a}$$

$$\omega N \to \pi N\,, \tag{3.5b}$$

$$\omega \to 3\pi\,. \tag{3.5c}$$

Cross section (a) is taken the same as for $\bar{K}$ elastic scattering at the same value of the c.m. energy; cross section (b) is obtained by detailed balance; for process (c) we use the free-space lifetime.

The pion momentum spectrum is hardly different from the resonance-free (without ω's) case (fig. 3); as for the multiplicities, the effect is rather small as can be seen from table 1. As already noticed in ref. [35]), the presence of ω's tend to shield pions from absorption. Since, however, only one "equivalent" pion in five is hidden in an ω, the global effect is small.

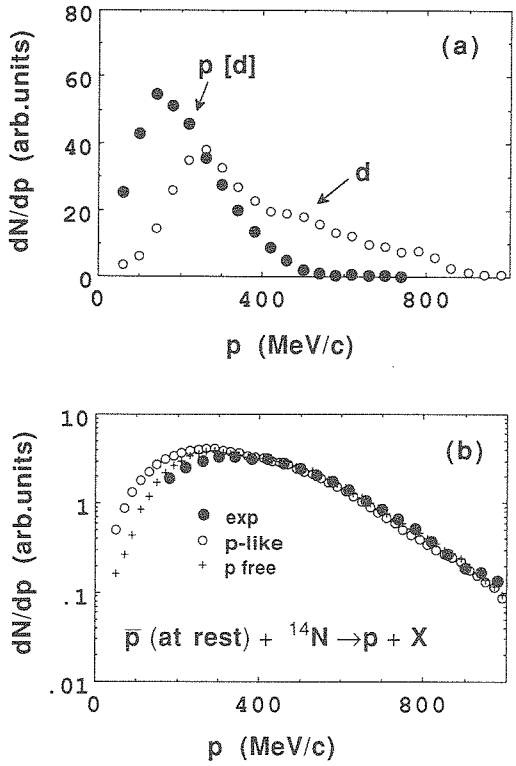

Fig. 5. Deuteron momentum distribution in $\bar{p}^{14}$N annihilation at rest (open dots, part (a)). The full dots in part (a) give the momentum distribution of the protons which have led to deuteron production. In part (b) is shown the effect on the proton spectrum: spectrum of all protons, free or hidden inside deuterons (open dots), spectrum of free protons (crosses) and experimental proton spectrum (full dots). See text for detail.

3.4. RATE OF Λ PRODUCTION

We have run the cascade with particular ingredients to find out if the observed Λ yield in ^{14}N can be accounted for by conventional mechanisms. The following conditions are used:

– the kaonic channels in $\bar{p}$N annihilation are included;

– hyperon production is obtained through (hyperon production by pions being negligible here):

$$\bar{K}N \to Y\pi, \tag{3.6a}$$

$$\omega N \to YK, \tag{3.6b}$$

and hyperon rescattering is included:

$$\Lambda N \leftrightarrow \Sigma N. \tag{3.7}$$

For reaction (3.6b), we used two different assumptions:

$$\sigma(\omega N \to YK) = (p_\pi^*/p_\omega^*)\sigma(\pi N \to YK)\,, \tag{3.8a}$$

as in ref. [35]), or

$$\sigma(\omega N \to YK) = \sigma(\pi N \to YK)\,, \tag{3.8b}$$

as in ref. [42]). The quantities p_π^*, p_ω^* are the c.m. momenta. The cross sections are taken at the same c.m. energy.

We take a potential of 30 MeV for the hyperons inside the nucleus. The fraction of events where the hyperon remains trapped (and will presumably undergo weak decay) is ≈30%. The predicted rates for strange particles are given in table 2. It is seen that our calculated rate of Λ production is greater than experiment. Even forgetting the ω contribution, the expected rate is a bit higher than the data, although assuming 4×10^{-2} instead of 5×10^{-2} for $K\bar{K}$ production would achieve good agreement. There are other uncertainties in the calculation (role of K*, possible breaking of the nucleus, ...) so that the discrepancy does not seem too serious.

For Ne, the measured Λ rate is also overestimated, but in this case the K_S rate has also been measured and allows a more complete and more general investigation (see sect. 4.3).

TABLE 2

Strange particle multiplicity (in 10^{-3}) for $\bar{p}$ annihilation at rest on ^{14}N (top) and on ^{20}Ne (bottom). The second column gives the primordial multiplicities and the third one, the contributions coming from the ω channels. The quantities σ_1 and σ_2 refer to the cross sections given by eqs. (3.8a) and (3.8b), respectively. The fourth column gives the contribution due to $\bar{K}$ channels and the fifth column, the total contribution. The Λ, Σ and $\tilde{\Lambda}$ multiplicities refer to free particles only. The mention "bound Y" corresponds to the hyperons which are captured by the target

Particle	Primordial	From ω channels		From $\bar{K}$ channels	Sum		Exp. [17,22])
		$\sigma_1(\omega)$	$\sigma_2(\omega)$		$\sigma_1(\omega)$	$\sigma_2(\omega)$	
K	50.0	5.4	3.4	50.0	55.4	53.4	
$\bar{K}$	50.0	0.0	0.0	35.32	35.32	35.32	
Λ		3.0	1.5	6.70	9.70	8.2	
Σ		1.2	1.2	3.45	4.65	4.65	
$\tilde{\Lambda} = \Lambda + \Sigma/3$		3.4	1.9	7.85	11.25	9.75	6.2±0.8
Bound Y		1.2	0.7	4.53	5.73	5.23	
$R = \tilde{\Lambda}/K_S$		2.52	2.24	0.37	0.50	0.44	
K_S		1.35	0.85	21.33	22.68	22.18	
K	50.0	7.0	3.7	50.0	57.0	53.7	
$\bar{K}$	50.0	0.0	0.0	34.17	34.17	34.17	
Λ		3.6	1.9	7.48	11.08	9.38	
Σ		1.7	0.9	3.48	5.18	4.38	
$\tilde{\Lambda} = \Lambda + \Sigma/3$		4.17	2.2	8.64	12.81	10.84	
Bound Y		1.7	0.9	4.87	6.57	5.77	
$R = \tilde{\Lambda}/K_S$		2.38	2.38	0.41	0.56	0.49	1.25±0.19
K_S		1.75	0.92	21.04	22.79	21.97	

4. The Λ/K_S ratio and related quantities

4.1. INTRODUCTION

Much emphasis has been put recently on this (easily measured) quantity with the suggestion that it signals strangeness enhancement. In ref. [14]), we showed in a particular case that this quantity is mainly sensitive to strangeness exchange processes. Below, we establish general relations, valid for symmetric systems, which show that at low energy, the Λ/K_S ratio is a simple function of the amount of strangeness exchange in rescattering. It is completely independent of the total strange yield which is given by some other quantities.

4.2. GENERAL RELATIONS FOR SYMMETRIC SYSTEMS

Let us assume that we have total charge symmetry. This would strictly correspond to the average on antiproton and antineutron interaction with a symmetric target. However, in annihilation channels, the production of several pions acts as a charge reservoir which largely removes the constraint of charge conservation.

At low energy, production of strange-particle species has three components: (a) direct production from annihilation; (b) strangeness exchange; (c) associated production by rescattering mesons. If we disregard the production of hyperons in the annihilation, it is quite easy to write down the following formulae for the final abundances of hyperons, kaons and antikaons, respectively

$$\langle Y\rangle = \kappa f_{SE} + f_{AP}\,, \tag{4.1a}$$

$$\langle K\rangle = \kappa + f_{AP}\,, \tag{4.1b}$$

$$\langle \bar{K}\rangle = \kappa - \kappa f_{SE}\,, \tag{4.1c}$$

where κ is the primordial rate of $K\bar{K}X$ annihilations, f_{SE} is the probability for strangeness exchange per primordial antikaon and f_{AP} is the contribution coming from associated production.

Going from eqs. (4.1) to abundances for different species is not straightforward, as this depends upon the distribution within a family. However, if we call α the fraction of hyperons appearing as $\tilde{\Lambda}$'s (defined as free Λ's and free Σ^0's), we can write

$$\langle \tilde{\Lambda}\rangle = \alpha\langle Y\rangle = \alpha[\kappa f_{SE} + f_{AP}]\,, \tag{4.2}$$

$$\langle K_S\rangle = \tfrac{1}{4}[\langle K\rangle + \langle \bar{K}\rangle] = \tfrac{1}{4}[2\kappa - \kappa f_{SE} + f_{AP}]\,. \tag{4.3}$$

The ratio $R = \langle\tilde{\Lambda}\rangle/\langle K_S\rangle$ is then given by

$$R = \frac{4\alpha(\kappa f_{SE} + f_{AP})}{2\kappa - \kappa f_{SE} + f_{AP}}\,. \tag{4.4}$$

At low energy, assuming associated production to be negligible, we have that R tends to R_{SE}

$$R_{SE} = 4\alpha f_{SE}/(2 - f_{SE}) . \tag{4.5}$$

The quantity α is different from (smaller than) unity, because of the presence of $\Sigma^{\pm}$ hyperons and because the Λ-particle can be captured by the nucleus. Therefore, at low energy, one has

$$R_{SE} \leqslant R_{lim} = 4f_{SE}/(2 - f_{SE}) . \tag{4.6}$$

At low energy, α lies around 0.5–0.6. Therefore, one can deduce that the $\tilde{\Lambda}/K_S$ ratio mainly measures the strangeness exchange probability in the rescattering process.

The strangeness content itself, defined as the abundance of strange (or antistrange) quarks

$$\langle s \rangle = \langle \bar{s} \rangle = \langle Y \rangle + \langle \bar{K} \rangle = \langle K \rangle \tag{4.7}$$

can be expressed as another combination of $\langle \tilde{\Lambda} \rangle$ and $\langle K_S \rangle$. Using

$$\langle s \rangle = \tfrac{1}{2}[\langle Y \rangle + \langle \bar{K} \rangle + \langle K \rangle] = \tfrac{1}{2}[\langle Y \rangle + 4\langle K_S \rangle] , \tag{4.8}$$

one obtains

$$\langle s \rangle = \langle \tilde{\Lambda} \rangle / 2\alpha + 2\langle K_S \rangle . \tag{4.9}$$

Note that (4.1) and (4.7) lead to

$$\langle s \rangle = \kappa + f_{AP} , \tag{4.10}$$

which simply indicates that strangeness is either created in the annihilation or by subsequent associated production.

Useful inequalities can be derived from the equations above. From (4.4), one gets

$$\alpha R_{lim} \leqslant R \leqslant 4\alpha , \tag{4.11}$$

where the factor 4 is the limiting value obtained when associated production only contributes, in a symmetric medium. From (4.1), one has

$$\langle K_S \rangle \geqslant \tfrac{1}{4}\kappa , \tag{4.12}$$

and finally, from (4.10), the obvious relation

$$\langle s \rangle \geqslant \kappa . \tag{4.13}$$

Similar expressions can be obtained for semi-exclusive yields. One readily obtains

$$\langle \tilde{\Lambda} K_S \rangle = \alpha(\tfrac{1}{4}\kappa f_{SE} + \tfrac{1}{4} f_{AP}) , \tag{4.14}$$

$$\langle K_S K_S \rangle = (1 - f_{SE})\{\tfrac{1}{16}\kappa + \tfrac{9}{64} f_{AP}\kappa\} . \tag{4.15}$$

These yields are semi-exclusive in the sense that they exclude any other strange particle than those which are explicitly stated, but they allow for any number of

accompanying non-strange particles. If associated production is unimportant, one gets

$$\frac{\langle \tilde{\Lambda} K_S \rangle}{\langle K_S K_S \rangle} = \frac{4\alpha f_{SE}}{1 - f_{SE}} . \tag{4.16}$$

One will notice the difference with formula (4.5), which, of course comes from correlations. We also obtain the relations

$$\frac{\langle K_S K_S \rangle}{\langle K_S \rangle} = \frac{1}{4}\left(\frac{1 - f_{SE}}{2 - f_{SE}}\right) \tag{4.17}$$

and

$$\frac{\langle \tilde{\Lambda} K_S \rangle}{\langle \tilde{\Lambda} \rangle} = \frac{1}{4} . \tag{4.18}$$

The ratio (4.17) is particularly interesting since it is independent of the primordial yield as $\tilde{\Lambda}/K_S$, but also of the factor α. The typical variation of both quantities, $\tilde{\Lambda}/K_S$ and (4.17), are illustrated in fig. 6.

4.3. EXPERIMENTAL VALUES OF $\langle \tilde{\Lambda} \rangle$, $\langle K_S \rangle$ AND R

In table 3, we summarize most of the known values of these quantities for several nuclei at rest (and at $p_{lab} = 0.6$ GeV/c for Ne). As expected, the ratio R roughly increases monotonically with the target mass in keeping with its direct relationship with strangeness exchange. The increase for the Ne target from the value at rest to

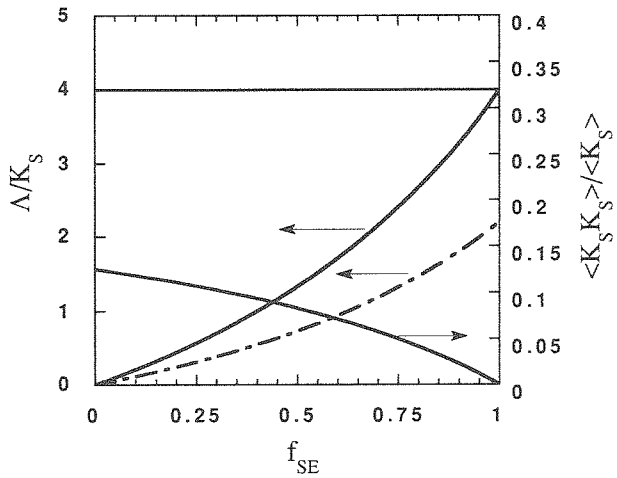

Fig. 6. Illustration of the variation of the $\tilde{\Lambda}/K_S$ for $\alpha = 1$ (eq. (4.5)) and $\langle K_S K_S \rangle / \langle K_S \rangle$ (eq. (4.17)) ratios with the strangeness exchange probability f_{SE}. The horizontal line gives the upper limit when associated production is present. The dot-dashed line correspond to the $\tilde{\Lambda}/K_S$ ratio with $\alpha = 0.55$. See text for detail.

TABLE 3

Experimental values. Strange particle yields after $\bar{p}$ annihilation at rest on light nuclei

Momentum	Target	$\langle\tilde{\Lambda}\rangle$ (10^{-3})	$\langle K_S\rangle$ (10^{-2})	$R=\langle\tilde{\Lambda}\rangle/\langle K_S\rangle$	Ref.
rest	p	-	2.37 ± 0.11	-	[21]
	n	-	2.50 ± 0.13	-	[21]
	d	3.0 ± 0.4	(2.43 ± 0.09)	0.22 ± 0.02	[17,21]
		3.6 ± 0.6		0.15 ± 0.08	[15,44]
	^{3}He	5.5 ± 1.1	1.59 ± 0.20	0.35 ± 0.08	[21,45]
	^{4}He	11.2 ± 1.2	1.07 ± 0.11	1.05 ± 0.16	[22,45]
	^{14}N	6.2 ± 0.8	-	-	[17]
	^{20}Ne	8.5 ± 1.5	0.72 ± 0.12	1.18 ± 0.29	[22,45]
600 MeV/c	^{20}Ne	19.5 ± 4.3	0.85 ± 0.17	2.3 ± 0.7	[10]

the value at 600 MeV/c is not an indication of new physics. It is merely due to the increase of the strangeness exchange probability as the annihilation site gets deeper and deeper into the nucleus. The limit of $\alpha R\approx 2.4$ (if α is taken ≈ 0.6) is obeyed. Values of R obtained at 3 and 4 GeV/c on a heavy nucleus (^{181}Ta) are not in contradiction with the same limit. Let us mention that associated production (and also $Y\bar{Y}$ primordial production) will tend to increase the value of R.

4.4. s-QUARK ABUNDANCE

This quantity can be expressed by eq. (4.9). Application of this formula is blurred by the limited knowledge of α. Detailed cascade calculations for ^{12}C and ^{20}N targets (see table 2) and simple estimate for ^{3}He show that α lies around 0.55. In these conditions, eq. (4.9), applied to the entries of table 3 when $\langle\tilde{\Lambda}\rangle$ and $\langle K_S\rangle$ abundances are determined independently (^{3}He, ^{4}He at rest, and ^{20}Ne at rest and at 600 MeV/c), gives $\langle s\rangle=(3.68\pm0.4)\%$, $(3.14\pm0.24)\%$, $(2.22\pm0.27)\%$ and $(3.47\pm0.52)\%$, respectively. Even by taking α as low as 0.5 for Ne, one finds 2.29 ± 0.28 and 3.65 ± 0.55. These numbers are really puzzling, since the final strange quark abundance is *smaller* than the usual quoted value for the primordial one ($\kappa\approx 4.5$-5%, see table 3). Apart from some possible misidentification in the V-tracks (but that would hardly be

TABLE 4

Branching ratios for two-body exit channels in $\bar{p}d$ annihilation at rest. The predictions of the second column are based on the statistical model calculation of ref. [8]) for the Σ^-K^+/π^-p ratio and on the experimental value of ref. [16]) for the π^-p yield: 28×10^{-6}. The work of ref. [5]) is based on the meson exchange picture

	Predicted [8])	Predicted [5])	Exp. (upper limit)
$\bar{p}d\to\Sigma^-K^+$	5×10^{-6}	1.1×10^{-8}-1.4×10^{-7}	8×10^{-6} [ref. [16])]
$\bar{p}d\to\tilde{\Lambda}K^0$	7×10^{-6}		"at the level of 10^{-5}" [ref. [17])]

sufficient to reconcile the numbers) or counting losses, the explanation should be that primordial annihilation has strangeness production properties which are different from those observed for free-space situation in bubble chambers. It may be due to the influence of the nuclear medium or, more simply, to the fact that in nuclear targets the $\bar{p}N$ annihilating state (where target nucleon N is the partner of the antiproton in the annihilation) is not the S-state which dominates in liquid hydrogen (and D) at rest. In that respect, let us recall that a decrease by the factor ≈ 3.8 has been observed for the yield of the exclusive $\bar{p}p \to K^+K^-$ channel when going from S- to P-wave $\bar{p}p$ annihilation at rest (with a decrease by the factor ≈ 5.7 in the $\pi^+\pi^-/K^+K^-$ ratio [43]). Although the rates of these channels are quite low ($\sim 10^{-3}$) the observed effect suggests that the operation of (dynamical) selection rules may influence significantly the output of the reaction depending on the initial state. This could translate in a decrease of κ when going from s-wave to higher l-wave annihilations.

At high energy, a similar analysis is not really conclusive since the primordial strange yields are not so well known. However, it seems [13,14]) that there is no strangeness enhancement either in this case.

4.5. CORRELATIONS

Semi-exclusive rates involving neutral strange particles have been recently measured for $\bar{p}^3$He at rest [21]), where one has $\langle \tilde{\Lambda} K_S \rangle = (1.5 \pm 0.8) \times 10^{-3}$ and $\langle K_S K_S \rangle = (2.0 \pm 0.9) \times 10^{-3}$. Although the statistical uncertainty is large, let us see whether the figures are consistent with the relations derived above. The $\langle \tilde{\Lambda} \rangle$ and $\langle \tilde{\Lambda} K_S \rangle$ rates are quite consistent with relation (4.18). The $\langle K_S K_S \rangle / \langle K_S \rangle$ ratio involves f_{SE}, which is not known. In principle, eq. (4.17) itself can be used to extract f_{SE}. Unfortunately, the dependence upon f_{SE} is weak and the experiment value of $\langle K_S K_S \rangle / \langle K_S \rangle$ is badly determined (incidentally, we notice that the average value is just consistent with the upper limit imposed by eq. (4.17)). However, we can estimate f_{SE} by means of the $\langle K_S \rangle$ rate, which has the smallest relative error. From eq. (4.3), putting $f_{AP} = 0$, and using $\kappa = 3.68 \pm 0.41$, the highest possible value according with the discussion of sect. 4.4, we get

$$f_{SE} = 0.27 \pm 0.18 \,. \tag{4.19}$$

The $\langle K_S K_S \rangle$ rate is predicted on this basis equal to $(1.7 \pm 0.4) \times 10^{-3}$. We thus find that, within the large uncertainties, the pattern of measured yields is consistent with a production of Λ's through strangeness exchange from primordial $\bar{K}$'s, the latter, however, being, produced with a rate lower (by $\sim 25\%$) than usually assumed at rest.

5. Summary and conclusions

The calculations reported in sects. 2 and 3 have been made on the basis of a semiclassical picture of $\bar{p}$ nucleus annihilations. We have analyzed annihilation on

^{2}H and ^{14}N, with special attention devoted to the possible role of $B = 1$ annihilations. We have defined such processes as those which are not relevant to a description where primordial mesons from a $B = 0$ annihilation on their mass shell are possibly rescattered by the nucleus.

In ^{2}H we have found that a high momentum component in the proton spectrum can be understood by the rescattering of one real annihilation pion on the "spectator". On the other hand, the presence of the π^-p channel is the signature of a genuine $B = 1$ process. If we rely on the predictions of a statistical model for $B = 1$ annihilations we find that $\approx$3% of the annihilations on ^{2}H at rest can be ascribed to such processes and that it should produce 1.7×10^{-3} Λ per event. As for $\bar{K}$ and ω rescattering, we estimate a contribution of $\sim 2.8 \times 10^{-3}$. These figures have to be compared with an observed $(3.0 \pm 0.4) \times 10^{-3}$. It must also be emphasized that the experimental information on the π^-p channel is somewhat contradictory [15-17]) and that a higher accuracy is awaited to draw more precise conclusions.

Turning to annihilations on N and Ne we have applied the INC model. The pion spectrum is fairly well reproduced as well as the pion multiplicity. However, the relative error on pion absorption is large so that the present result is not a very precise test of the ability of the cascade to reproduce pion absorption in nuclear matter. In the ^{14}N case, the model predicts $\approx$40% of the primordial pions to interact and $\approx$40% of these to be absorbed. We recall that some deficit in pion absorption was found in a survey of results for a large range of A values, the data being, however, rather scattered. We find that each interacting pion ejects, on the average, 1.32 protons, giving a total of 2.51. This is somewhat larger than the experimental count: for momentum >170 MeV/c, the figures are: 0.9 predicted for (0.7 ± 0.03) detected. But using a simple coalescence model we could fit nicely the heavy positive spectrum.

We have also looked at the role of the ω-meson, a long-lived resonance whose yield in primordial annihilation is quite noticeable. We have found that, with the retained assumption for its interaction properties, its coming into play does not modify much the output of the pionic cascade. Understandably, it works in the direction of a reduction of pion absorption (by $\approx$15%). This remains within the experimental uncertainties.

Hyperon production in meson rescattering has been computed. Production by pions is completely negligible for annihilation at rest compared to production by $\bar{K}$ (through strangeness exchange) and ω. The predicted yield for Λ in N is rather larger than observed.

We enlarge the discussion on strange-particle yield in sect. 4. In particular, we showed *on very general grounds* that the Λ/K_S ratio mainly measures the strangeness exchange process induced by the primordial antikaons and is *not* an indicator of the final strangeness yield and therefore cannot signal a possible strangeness enhancement. The total strangeness yield is carried by another quantity $(\frac{1}{2}\langle\tilde{\Lambda}\rangle + 2\langle K_S\rangle)$, which, of course, is not sensitive to strangeness exchange. We also derive

general inequalities between strangeness related quantities, and for semi-exclusive quantites, which can be used as a consistency check for experimental data. We showed that for ^{3}He, ^{4}He and ^{24}Ne, there seems to be an *inhibition* and not an enhancement of strangeness production; this is particularly obvious for $\bar{p}$Ne at 600 MeV/c. These results strongly emphasize the need for further and *precise* measurements; in particular measurements of charged K's and Σ's are desirable. A possible explanation of the inhibition in terms of dynamical selection rules has been presented.

We would like to thank Dr. J. Riedlberger for having provided us with details about the ASTERIX experiment and Dr. C. Guaraldo for useful discussions.

References

1) J. Rafelski, Phys. Lett. **B91** (1980) 281
2) J. Rafelski, Phys. Lett. **B207** (1988) 371
3) S. Kahana, Proc. Workshop on Physics at LEAR, ed. U. Gastaldi and R. Klapisch (Plenum, New York, 1984) p. 485
4) J. Cugnon and J. Vandermeulen, Phys. Lett. **B146** (1984) 16
5) E. Hernandez and E. Oset, Phys. Lett. **B184** (1987) 1
6) L.A. Kondratyuk and M.G. Sapozhnikov, Physics at LEAR with low energy antiprotons, ed. C. Amsler *et al.* (Harwood, Chur, 1988) p 771
7) L. Kondratyuk and C. Guaraldo, CERN-EP/89-122 (submitted to Nucl. Phys. A)
8) J. Cugnon and J. Vandermeulen, Phys. Rev. **C39** (1989) 181
9) J. Cugnon and J. Vandermeulen, Phys. Rev. **C36** (1986) 2726
10) F. Balestra *et al.*, Phys. Lett. **B194** (1987) 1982
11) K. Miyano *et al.*, Phys. Rev. **C38** (1988) 2788
12) C.B. Dover and P. Koch, Invited talk at the Conf. on hadronic matter in collision, Tucson, Arizona, Oct. 1988 and preprint BNL-42105
13) W.R. Gibbs and J.W. Kruk, Phys. Lett. **B237** (1990) 317
14) J. Cugnon, P. Deneye and J. Vandermeulen, Phys. Rev. **C41** (1990) 1701
15) R. Bizzarri *et al.*, Lett. Nuovo Cim. **2** (1969) 431
16) G.A. Smith, in The elementary structure of matter, ed. J.-M. Richard *et al.*, (Springer, Berlin, 1988) p. 219
17) J. Riedlberger *et al.*, Phys. Rev. **C40** (1989) 2717
18) J.-P. Bocquet *et al.*, Phys. Lett. **B182** (1986) 146; **B192** (1987) 312
19) S. Polikanov, Nucl. Phys. **A478** (1988) 805c
20) M. Rey-Campagnolle, Nuovo Cim. **102A** (1989) 653
21) Y.A. Batusov *et al.*, Dubna preprint E1-90-118
22) C. Guaraldo, CERN-EP/89-87
23) S.C. Phatak and N. Sarma, Phys. Rev. **C36** (1987) 864
24) A.S. Iljinov, V.I. Nazaruk and S.E. Chigrinov, Nucl. Phys. **A382** (1982) 378
25) P. Jasselette, J. Cugnon and J. Vandermeulen, Nucl. Phys. **A484** (1988) 542
26) J. Cugnon, P. Deneye and J. Vandermeulen, Nucl. Phys. **A500** (1989) 701
27) J. Rafelski, Proc. Workshopon Physics at LEAR, ed. U. Gastaldi & R. Klapisch (Plenum, New York, 1984)
28) L. Hulthén and M. Sugawara, Handbuch der Physik **39** (1957) 1
29) M. Lacombe, B. Loiseau, J.-M. Richard, R. Vinh Mau, J. Côté, P. Pirès and R. De Tourreil, Phys. Rev. **C21** (1980) 861
30) E.C. Fowler, T.D. Taft and E.R. Mosburg, Phys. Rev. **106** (1957) 829

31) P.D. Zemany, Z. Ming Ma and J.M. Mountz, Phys. Rev. Lett. **38** (1977) 1443
32) G. Levman *et al.*, Phys. Rev. **D21** (1980) 1
33) J. Roy, Proc. IV Int. Symp. on nucleon–antinucleon interactions, Syracuse, (1975) p. III-1
34) M.P. Locher, Int. Conf. on medium- and high-energy nuclear physics, Taipei, R.O.C.
35) J. Cugnon, P. Deneye and J. Vandermeulen, Phys. Rev. **C40** (1989) 1822
36) J. Cugnon, P. Deneye and J. Vandermeulen, Nucl. Phys. **A513** (1990) 636
37) J. Cugnon, P. Deneye and J. Vandermeulen, Phys. Rev. **C38** (1988) 795
38) Ye.S. Golubeva, A.S. Iljinov, A.S. Botvina and N.M. Sobelevsky, Nucl. Phys. **A483** (1988) 539
39) G.A. Smith, Hyp. Int. **44** (1988) 43
40) A. Schwarzschild and C. Zupancic, Phys. Rev. **129** (1963) 854
41) H.H. Gutbrod *et al.*, Phys. Rev. Lett. **37** (1976) 854
42) H. Bando and J. Zofka, Phys. Lett. **B241** (1990) 7
43) M. Doser *et al.*, Nucl. Phys. **A486** (1988) 493
44) S.H. Parkin *et al.*, Nucl. Phys. **B227** (1986) 634
45) F. Balestra *et al.*, submitted to Nucl. Phys.